Post-injury immunosuppression and secondary infections are caused by an AIM2 inflammasome-driven signaling cascade

Stefan Roth[1], Jiayu Cao[1], Vikramjeet Singh[1], Steffen Tiedt[1,2], Gabriel Hundeshagen[3], Ting Li[4], Julia D Boehme[5,6], Dhruv Chauhan[7], Jie Zhu[1], Alessio Ricci[1], Oliver Gorka[8], Yaw Asare[1], Jun Yang[1], Mary S. Lopez[1], Markus Rehberg[1], Dunja Bruder[5,6], Shengxiang Zhang[4], Olaf Groß[8,9,10], Martin Dichgans[1,2], Veit Hornung[7], Arthur Liesz[1,2]*

1 Institute for Stroke and Dementia Research (ISD), University Hospital, LMU Munich, Munich, Germany

2 Munich Cluster for Systems Neurology (SyNergy), Munich, Germany

3 Department of Hand-, Plastic and Reconstructive Surgery, Burn Center, BG Trauma Center Ludwigshafen, University of Heidelberg, Ludwigshafen, Germany.

4 Gansu Key Laboratory of Biomonitoring and Bioremediation for Environmental Pollution, School of Life Sciences, Lanzhou University, Lanzhou, China

5 Immune Regulation, Helmholtz Centre for Infection Research, Braunschweig, Germany.

6 Infection Immunology, Institute of Medical Microbiology, Infection Control and Prevention, Health Campus Immunology, Infectiology and Inflammation, Otto von-Guericke University, Magdeburg, Germany.

7 Gene Center and Department of Biochemistry, Ludwig-Maximilians-Universität München, Munich, Germany.

8 Institute of Neuropathology, Medical Center – University of Freiburg, Freiburg, Germany

9 Signalling Research Centres BIOSS and CIBSS, Freiburg, Germany

10 Center for Basics in NeuroModulation (NeuroModulBasics), Freiburg, Germany

*To whom correspondence should be addressed: arthur.liesz@med.uni-muenchen.de

Summary

Loss of lymphocytes, particularly T cell apoptosis, is a central pathological event after severe tissue injury which is associated with increased susceptibility for life-threatening infections. The precise immunological mechanisms leading to T cell death after acute injury are largely unknown. Here, we identified a monocyte-T cell interaction driving bystander cell death of T cells in ischemic stroke and burn injury. Specifically, we found that stroke induced a FasL-expressing monocyte population, which led to extrinsic T cell apoptosis. This phenomenon was driven by the AIM2 inflammasome-dependent interleukin-1β (IL-1β) secretion after sensing cell-free DNA. Pharmacological inhibition of this pathway improved T cell survival and reduced post-stroke bacterial infections. As such, this study describes inflammasome-dependent monocyte activation as a previously unstudied cause of T cell death after injury, and challenges the current paradigms of post-injury lymphopenia.

Introduction

Extensive tissue injuries including stroke, trauma, and major surgeries commonly induce a period of marked immunosuppression similar to sepsis-induced immunosuppression (Lord et al., 2014; Meisel and Meisel, 2011). Immunosuppression after injury is primarily characterized by a rapid and massive loss of T cells due to apoptosis (Chamorro et al., 2012; Girardot et al., 2017; Lord et al., 2014), which predisposes patients with local tissue injuries to systemic infections. In fact, infections are a major cause of death after sterile tissue injuries (D'Avignon et al., 2010; Meisel and Meisel, 2011). However, the mechanisms leading to T cell apoptosis after sterile tissue injury remain largely elusive.

The currently prevailing concepts assume either T cell autonomous mechanisms or the stress response to tissue injury as the most likely cause of T cell death and immunosuppression (Hotchkiss et al., 2013; Meisel et al., 2005; Woiciechowsky et al., 1998). However, both concepts have recently been mechanistically challenged (Hotchkiss et al., 2013; Rubio et al., 2019) and, despite over two decades of intense effort and an enormous medical need, these approaches did not result in a drug reaching approval to target post-injury T cell apoptosis in patients.

We focused on a conceptually different approach: the role of soluble blood factors in mediating extrinsic apoptosis of T cells. The activation of extrinsic T cell apoptosis is initiated by membrane-bound death receptors after ligand binding (Fas et al., 2006). Activation of death receptors results in caspase-8 dependent programmed cell death. In contrast to intrinsic apoptosis—induced by mitochondrial outer membrane permeabilization, generally in response to cellular dysfunction—the extrinsic apoptosis cascade can be either induced cell-autonomously after T cell activation or non-autonomously by other cells or soluble death receptor ligands. Extrinsic T cell apoptosis plays an

important physiological role in development, regulating homeostasis of the cell population and in contraction of T cell immune responses (Bouillet and O'Reilly, 2009).

The predominant phenomenon of post-injury lymphopenia is preceded by a pro-inflammatory response in the hyperacute phase within the first hours after tissue injury. During this initial phase high concentrations of cytokines can be measured in blood of patients with severe injuries (Finnerty et al., 2006; Lambertsen et al., 2012; Liesz et al., 2015; Ormstad et al., 2011). Therefore, we questioned whether the initial cytokine storm after injury might be causally related to the subsequent T cell apoptosis by potentially inducing extrinsic cell death via currently unknown mechanisms.

In this study we used for the majority of our experiments an experimental stroke model as a prototypic tissue injury model, which we and others have previously shown to result in pronounced lymphopenia with loss of >50% of T cells (Liesz et al., 2009a; Liesz et al., 2009b; Meisel et al., 2005). Key findings from the stroke model were generalizable to a second tissue injury model of burn lesions. Finally, analysis of a large cohort of stroke patients and two experimental post-injury infection models revealed a key role of the this previously unrecognized pathway along inflammasome-dependent monocyte activation and FasL-Fas-mediated T cell apoptosis for subacute infections.

T cell apoptosis occurs as bystander cell death following injury-induced FasL$^+$ myeloid cells

We aimed to test the hypothesis that soluble mediators released after injury are a potential cause for T cell apoptosis. First, we confirmed a pronounced and general T cell death across subpopulations after experimental stroke which occurred even under sterile (germfree) conditions, hence, cannot be attributed to potential concomitant microbial infections (Suppl. Fig. 1). Next, we utilized a murine parabiosis model in which only one parabiont received either a stroke or sham operation (Suppl. Fig. 2A, B, confirming full chimerism in all mice) and observed a significant reduction of splenic T cells after stroke in the operated animal as well as in the non-operated parabiont, indicating that blood factors and not neuronal innervation plays a crucial role in this phenomenon (**Fig. 1A**). Therefore, we used the serum of stroke- or sham-operated mice for the further *ex vivo* analysis of T cell death by treating freshly isolated mixed splenocytes or purified T cells. Whole splenocytes incubated with stroke serum showed significantly reduced T cell viability, supporting the concept that cytotoxic factors circulate in the blood after stroke (**Fig. 1B**). However, incubation of purified T cells with serum from either sham- or stroke-operated mice did not affect T cell survival, indicating that T cell non-autonomous mechanisms lead to T cell apoptosis (**Fig. 1B**). Importantly, serum catecholamine concentrations at this early stage after stroke were not altered (Suppl. Fig. 2C, D) and *in vivo* treatment with β2-adrenoreceptor inhibitors did not affect T cell survival in spleens after stroke (Suppl. Fig. 2E). This, in conjunction with the results of the parabiosis experiments, challenges the previously suggested concept of adrenoreceptor-dependent T cell death (Prass et al., 2003) at this early time point after stroke. In light of these findings, we speculated whether post-injury T cell death might instead

occur as a bystander phenomenon to activation of cells other than T cells by injury-released blood factors. To this end, we first turned our attention to the myeloid cell compartment and established *in vitro* co-culture models of bone-marrow derived macrophages (BMDMs) and T cells with and without cell contact (**Fig. 1C**). Stroke serum-mediated activation of BMDMs induced T cell death only with direct cell-cell contact with BMDMs, whereas supernatant from serum-stimulated BMDMs was not cytotoxic for T cells (**Fig. 1D**). These findings indicated that myeloid cells exerted a cytotoxic function on T cells, induced by soluble factors in the post-injury serum. Non-autonomous T cell death was further corroborated by the finding that inhibiting the extrinsic caspase-8- but not intrinsic caspase-9-dependent apoptosis prevented T cell death (Suppl. Fig. 2F). Extrinsic apoptosis of T cells can be mediated by various cell-surface receptors of the tumor necrosis factor (TNF) family, of which Fas (CD95) is a prototypical death receptor (Krammer et al., 2007). Multiparametric flow cytometry analysis revealed a FasL-positive subpopulation of tissue injury-induced monocytes (TIM) after experimental stroke (**Fig. 1E**). Treatment of mixed splenocytes—which allows an unbiased ex vivo analysis of all splenic leukocyte subpopulations and their potential interactions—with stroke serum *in vitro* revealed a close temporal association between the monocytic FasL upregulation and T cell death (Suppl. Fig. 2G, H). Correspondingly, treatment of mice with FasL-specific neutralizing antibodies significantly improved T cell survival post-injury (**Fig. 1F**). Hence, we tested the role of the death receptor Fas in extrinsic T cell death by comparing WT and Fas-deficient (Fas^{lpr}) T cells first in an *in vitro* co-culture with serum-stimulated BMDMs. Indeed, Fas-deficient T cells were protected from the cytotoxic effect of stroke serum-stimulated monocytes (**Fig. 1G**). Next, we aimed to validate this finding *in vivo* by adoptively transferring Fas^{lpr} or WT T cells to lymphocyte-deficient *Rag-1*$^{-/-}$ mice. In contrast to WT T cells, post-stroke cell death was completely prevented in Fas^{lpr} T cells, demonstrating the critical role of Fas-signaling for post-stroke T cell death (**Fig. 1H**). Of note, neither the anti-FasL treatment nor Fas-deficiency on T cells directly affected the infarct volume (Suppl. Fig. 2I, J). In summary, these experiments reveal a previously unrecognized cause of post-injury lymphopenia: extrinsic T cell apoptosis as bystanders to an injury-induced $FasL^+$ myeloid population.

T cell cytotoxic FasL upregulation on monocytes is mediated by post-injury IL-1β secretion

To determine the circulating mediators leading to induction of the $FasL^+$ myeloid cell population, we performed a multiplex assay for cytokines and chemokines in the serum of mice 6h after sham or stroke surgery, which identified interleukin-1β (IL-1β) as the most abundantly upregulated cytokine (**Fig. 2A**). In order to test a causative role of increased post-injury IL-1β concentrations for FasL expression on myeloid cells and T cell death, we stimulated BMDMs with recombinant IL-1β . This experiment showed increased FasL expression on BMDMs and increased T cell death in a BMDM-T cell coculture when treated with recombinant IL-1β in comparison to control treatment (**Fig. 2B**). Correspondingly, the *in vivo* neutralization of IL-1β by monoclonal antibodies completely blunted the

induction of the FasL$^+$ myeloid cell population (**Fig. 2C**). Moreover, neutralizing circulating IL-1β by IL-1β–specific antibodies significantly improved T cell survival after stroke (**Fig. 2D**). In turn, the injection of recombinant IL-1β to mice dose-dependently induced T cell death and FasL upregulation on myeloid cells, closely resembling the stroke-induced phenotype (**Fig. 2 E, F**). Taken together, these experiments reveal that the post-injury increase in IL-1β blood concentration drives the expansion of T cell-cytotoxic FasL$^+$ myeloid cells.

IL-1β driven T cell death is inflammasome dependent

Caspase-1, the central effector enzyme of the inflammasome, tightly regulates both cleavage of pro-IL-1β and extracellular release of mature IL-1β (Guo et al., 2015). Correspondingly, we found that local tissue injury in mice increased the amount of splenic pro-caspase-1 and active cleavage isoforms, indicating systemic post-stroke inflammasome activation (**Fig. 3A**). We corroborated this result by staining post-stroke spleens with FAM FLICA, a fluorescent molecule that selectively binds activated caspase-1 (Suppl. Fig. 3A). In order to test the effect of circulating blood factors on inflammasome activation and IL-1β release in human cells, we cultured human peripheral monocytes from healthy donors and treated the cells with serum from either stroke or healthy patients (see methods section for details of the culture system). We detected a consistent increase in caspase-1 cleavage and secretion of IL-1β from these cultured monocytes in the stroke serum conditions as compared to the control (**Fig. 3B**, Suppl. Fig. 3B). These findings demonstrate that circulating factors released after local tissue injury lead to systemic inflammasome activation and IL-1β release. In order to further specify the cellular identity of inflammasome activation—the source of IL-1β—we performed flow cytometry imaging in ASC-citrine mice, a reporter strain for visualizing inflammasome assembly (Tzeng et al., 2016) and detected inflammasome formation in splenic monocytes (**Fig. 3C**). In a series of *in vivo* experiments using different transgenic models of inflammasome-deficiency, we were able to confirm the concept of inflammasome-dependent IL-1β secretion from splenic monocytes as the driver of FasL-mediated T cell death. This approach showed that global deficiency for caspase-1 and the adaptor molecule ASC (*Pycard*) ameliorated post-injury T cell death (**Fig. 3D**, Suppl. Fig. 3C). Moreover, inflammasome deficiency completely prevented the increase in post-injury IL-1β secretion and FasL expression (Suppl. Fig. 3D, E). Conditional inflammasome deficiency only in the myeloid cell compartment (using *Lyz2-cre x Pycard$^{fl/fl}$* mice) was sufficient to completely rescue post-injury T cell death (**Fig. 3E**), demonstrating the critical role of monocytic inflammasome activation for T cell death. We further investigated the specificity of IL-1β in this phenomenon, specifically in comparison to the closely related IL-1α and to IL-18. While also IL-1α and IL−18 were increased in serum after stroke, FasL upregulation on myeloid cells was predominantly induced by IL-1β (Suppl. Fig. 3G).

Peripheral monocytes sense injury-released cell-free DNA by the AIM2 inflammasome

Since our results demonstrated that inflammasome activation in monocytes is the upstream causative mediator of IL-1β driven T cell death, we next aimed to identify the specific type of inflammasome and corresponding ligand involved in this process. While some inflammasome sensors respond to specific pathogen-derived factors, other sensors can be engaged by self-molecules that are released upon cell damage or are activated by certain breaches of cellular integrity (Hornung et al., 2009; Latz et al., 2013). We detected a significant increase in cell free double stranded DNA (cf-dsDNA) after stroke in mice and humans (**Fig. 4A, B**). Correspondingly, mice treated with 1000U of human recombinant DNase (hrDNase) showed reduced cf-dsDNA concentration in the blood (**Fig. 4C**), which substantially reduced inflammasome activation in splenic monocytes, prevented the expansion of the $FasL^+$ myeloid cell population, and improved T cell survival after experimental stroke (**Fig. 4D-F**). We further validated the causal function of cf-dsDNA for the induction of $FasL^+$ monocytes *in vitro*: ex vivo treatment of post-stroke mouse serum with hrDNAse did not affect the serum concentration of IL-1β but completely prevented the FasL upregulation on serum-stimulated monocytes (Suppl. Fig. 4A, B), showing that cf-dsDNA as the initial stimulus upstream of the IL-1β-induced FasL upregulation. We have previously shown that DNA binding to absent in melanoma 2 (AIM2) can lead to inflammasome activation in myeloid cells (Hornung et al., 2009). Accordingly, we observed a significant reduction in monocytic caspase-1 activation as well as drastically improved T cell death in *Aim2*$^{-/-}$ compared to WT mice (**Fig. 4G, H**). *In vitro* co-culture experiments confirmed the monocyte and AIM2 dependent, non-autonomous T cell death, such that *Aim2*$^{-/-}$ BMDMs stimulated with serum from stroke mice did not induce T cell death as compared to stroke serum-treated WT BMDMs (**Fig. 4I**). Notably, while the used genetic and pharmacological models to block AIM2 inflammasome activation efficiently prevented myeloid FasL upregulation, the primary lesion size was unaffected by these approaches. These results underscore the notion that the inflammasome pathway impacts on the systemic, immunological events following stroke rather than modulating lesion severity (Suppl. Fig. 4C, D). While we identified this monocyte-T cell interaction in the prototypic tissue injury model of brain ischemia, we were able to replicate all key events of this pathway—cf-dsDNA release, inflammasome activation, and subsequent T cell apoptosis—in an independent model of burn injury (Suppl. Fig. 5).

Inflammasome-driven lymphocyte death predisposes to bacterial infections

Patients with severe tissue injuries after stroke, trauma, or burn have a high susceptibility to infections, which contribute substantially to secondary mortality (D'Avignon et al., 2010; Meisel and Meisel, 2011). Therefore, after identifying the mechanism of T cell death by a bystander mechanism to inflammasome activation in monocytes, we aimed to test the relevance of this pathway for post-injury infections. We analyzed 174 patients with ischemic stroke for which complete information was

available for serum concentrations of dsDNA and IL-1β at hospital admission (d0; mean time after symptom onset: 4.9 hours), their blood lymphocyte counts on the subsequent day (d1) and the occurrence of infections (requiring antibiotic treatment and CRP >30 mg/l and/or radiographic confirmation) between days 2-7 after stroke onset (**Fig. 5A**). We detected a significant association between serum dsDNA and IL-1β concentrations as well as a significant negative association between IL-1β concentration on admission and blood lymphocyte counts on the following day (**Fig. 5B**). Patients with secondary infections after stroke showed significantly increased IL-1β concentrations on admission and reduced lymphocyte counts on d1 (**Fig. 5C**). Therefore, we performed a mediation analysis to test whether lymphocyte counts mediate the effect of IL-1β on the incidence of secondary infections. Supporting our hypothesis, acute IL-1β concentrations were significantly associated with subacute infections, where this effect was mediated via a reduction of lymphocyte counts. This effect was considered a full mediation because the direct effect of IL-1β concentrations on infections ($p=0.037$) was no longer statistically significant after inclusion of the mediator in the regression model ($p=0.12$) (**Fig. 5D**). Next, we aimed to test the therapeutic targeting of this pathway for immunocompetence during post-injury infections. Therefore, mice were treated with the pharmacological inflammasome inhibitor VX765 after stroke, which improved T cell survival (**Fig. 5E**). Then, VX765 or control-treated animals received an experimental respiratory tract infection with either *Streptococcus pneumoniae* or *Klebsiella pneumoniae* 12h after sham or stroke surgery and the bacterial load in the respiratory tract was analyzed another 14h later (**Fig. 5F**). Control-treated mice showed increased bacterial loads after stroke compared to sham surgery in both experimental pneumonia models, while inflammasome inhibition by VX765 reduced post-injury bacterial load comparable to sham-operated group (**Fig. 5G**). These findings reveal that inhibition of the inflammasome after stroke functionally increases immunocompetence by rescuing post-stroke T cell death instead of inhibiting the direct anti-microbial functions of inflammasome activation.

Discussion

Here we have identified a previously unrecognized mechanism of post-injury T cell death. We propose that inflammasome activation in myeloid cells and the subsequent expression of FasL on monocytes is the main cause of pronounced lymphopenia after stroke and burn injury. This cell death mechanism is dependent on the induction of a FasL-expressing monocyte population by IL-1β. While most activated lymphocytes express Fas on the cell surface, its interaction with FasL and induction of downstream extrinsic apoptosis is tightly controlled by multiple checkpoints, mainly on the side of FasL surface expression and trimerization for efficient Fas ligation (Li-Weber and Krammer, 2003; Strasser et al., 2009). This mechanism has been widely studied in cell-autonomous T cell apoptosis with implications for physiological T cell turnover, tumor immunity, and autoimmune disease (Krammer et al., 1994; Li-

Weber and Krammer, 2003). Despite the ubiquity of this cell death pathway in physiology and disease, the non-autonomous bystander cell death of T cells via FasL on myeloid cells has previously not been tested. Importantly, concordant results from two independent and pathophysiologically largely different animal models of acute tissue injury, stroke and burn injury, suggest the generalizability of the here identified signaling cascade across disease entities of acute tissue injury resulting in secondary immunosuppression. Besides the closely related trauma and myocardial infarction-induced immunosuppression, also tumor growth or the rapid cell death during tumor debulking (by chemotherapy or radiation) need to be considered as relevant pathomechanisms in which inflammasome-driven extrinsic T cell death might be the cause of secondary immunosuppression (Ayasoufi et al., 2020; Kroemer et al., 2013).

Our finding that IL-1β-induced FasL expression on monocytes is in line with previous studies in viral infection models, which demonstrated that monocytes express FasL in response to infection (Dockrell et al., 1998). Our study shows that *de novo* induction of a FasL-expressing monocyte population is driven by post-injury IL-1β secretion. *In vitro* treatment with rIL-1β is sufficient to induce $FasL^+$ monocytes, and *in vivo* neutralization efficiently prevented this effect. While it was, to our knowledge, not previously shown how exactly IL-1β induces FasL expression on monocytes, it is most likely that this is due to induction of the AP-1 complex leading to increased transcription of FasL in IL-1β-stimulated monocytes (Li-Weber and Krammer, 2003).

These results challenge previous concepts regarding how tissue injury leads to immunosuppression due to T cell death. Stress pathways and cell autonomous T cell death were commonly proposed as the cause of immunosuppression after acute tissue injury (Lord et al., 2014; Meisel and Meisel, 2011). This concept is based on the well-established effects of stress hormones on T cell function and was further supported by demonstrating beneficial effects of beta-blocker and glucocorticoid receptor inhibitor treatment on T cell survival after stroke and trauma (Barlow, 1994; Prass et al., 2003; Pruss et al., 2017). However, blood concentrations of catecholamines and cortisol in the blood of stroke, sepsis, and trauma patients are much lower than previously shown to be cytotoxic for T cells (Huang et al., 2013; Liesz et al., 2013; Mracsko et al., 2014; Norbury et al., 2008). Finally, none of the clinical trials of beta-blocker treatment on patients with stroke, trauma, or major surgery showed any benefits with regard to lymphopenia or secondary infections (Brinkman et al., 2014; Loftus et al., 2016; Westendorp et al., 2016). Here, our results from the parabiosis model and serum treatment of splenocytes show that neuronal innervation (autonomic nervous system) is not required, but soluble blood mediators are sufficient. Moreover, catecholamine concentrations are not yet increased in the first hours after stroke when inflammasome activation and T cell death can already be observed; and the inhibition of β2-adrenoreceptors—the catecholaminergic receptors expressed on T cells—did not affect acute T cell apoptosis. The post-injury serum did not have direct cytotoxic effects on T cells in absence of co-stimulatory myeloid cells. In conjunction, this clearly demonstrates that neither neuronal

innervation nor stress hormones in the serum are directly contributing to T cell death in the early phase after tissue injury.

In contrast to previous reports, inflammasome inhibition did not affect the primary tissue injury (i.e. infarct volume) in the acute time frame of less than 24h post-injury in which the peripheral immune-consequences were observed. However, previous studies that have suggested a potential neuroprotective effect of post-stroke inflammasome inhibition have investigated later time points after stroke (Denes et al., 2015; Poh et al., 2019). Therefore, additional protective functions of preventing inflammasome activation after tissue injury by reducing inflammation and secondary tissue injury at the primary lesion site cannot be excluded. In such a case inflammasome-inhibition after tissue injury not only would prevent immunosuppression and increased risk for life-threatening infections but also reduce the primary disease burden. Future studies will have to address this intricate relationship between systemic immune consequences and local tissue inflammation after injury.

The pathway identified here along the events of increased cf-dsDNA concentration, inflammasome activation, IL-1β secretion, and Fas-mediated T cell death provides several therapeutic targets for which currently available drugs could be repurposed. The results from our human substudy investigating a stroke patient cohort confirmed a strong association along this pathway which is mediating the occurrence of subacute infections in stroke patients. However, an important limitation of our clinical analysis is that this was based on a retrospective biomarker study and was not prospectively designed and powered; therefore, we cannot exclude other potential confounders to the increased infection rate in patients with higher dsDNA and IL-1β concentrations. Future prospectively designed clinical trials will have to validate the value of early dsDNA detection as a predictive biomarker of subacute lymphopenia and infection. The potential druggability of this pathway has been proven by our results demonstrating improved bacterial clearance after subacute respiratory tract infection when blocking the initial inflammasome activation. While this mechanistic study has identified several potential therapeutic targets to reduce the systemic immune-consequences of tissue injury, the robustness of these findings and there translational relevance should be validated in a fully-powered, preclinical confirmatory study before future attempts to clinical translation (Kimmelman et al., 2014; Llovera et al., 2015; Llovera and Liesz, 2016).

Besides direct blockage of the inflammasome by small molecules, a promising therapeutic target seems to be the pathological initiator of this immunological cascade, the increase in circulating cf-dsDNA. While the mechanisms of cf-dsDNA internalization of myeloid cells are still largely unknown, our current study shows that efficient degradation of cf-dsDNA via human recombinant DNase reduces post-stroke lymphopenia. Inhalable hrDNase is currently in clinical use for patients with cystic fibrosis (Fuchs et al., 1994), however, systemic administration and its effect on immunological events after tissue injury have not yet been assessed. Additionally, the IL-1β cytokine, the key inflammasome effector molecule, represents another promising drug target. We show in our experimental models that IL-1β secretion was sufficient for inducing the T cell cytotoxic $FasL^+$

monocyte population and in our clinical substudy that IL-1β predicted subacute infections via a reduction of lymphocyte counts. Hence, neutralizing circulating IL-1β with biologics may paradoxically improve systemic immune competence after tissue injury by preventing T cell death, despite being currently used as an immunosuppressive drug. Indeed, while IL-1β blockade was initially developed for rare autoimmune disorders, this approach has recently been tested for patients with myocardial infarction. IL-1β blockade significantly lowered recurrent local cardiovascular events in a large clinical trial (Ridker et al., 2017) and its local anti-inflammatory effects might reduce the development of heart failure (Panahi et al., 2018). However, the potential of this approach and its safety have so far not been clinically tested for the prevention of systemic immune alterations and associated comorbidities after acute tissue injuries.

Taken together, our study challenges current concepts and suggests a previously unrecognized mechanism of T cell death as the cause of immunosuppression after severe injuries. Identification of therapeutic targets along this pathway opens up new avenues for drug development and repurposing. Clinical studies are now required to test the efficacy of inhibiting T cell death to reduce infections and mortality in patients with severe tissue injuries.

Acknowledgements

The authors would like to thank Kerstin Thuß-Silczak for technical support and Daniela Maurer for help in immunoblotting. The authors are grateful to Eicke Latz (Institute of Innate Immunity, University Bonn, Germany) for providing *Aim2*$^{-/-}$ mice. We acknowledge the Core Facility Flow Cytometry at the Biomedical Center, Ludwig-Maximilians-Universität München, for providing equipment, services and expertise.

This work was funded by the Vascular Dementia Research Foundation. , the European Research Council (ERC-StGs 802305 to AL and 337689 to OG and ERC-CoG 647858 to VH), the National Natural Science Foundation of China (#31600831 and #81771324) and the German Research Foundation (DFG) under Germany´s Excellence Strategy (EXC 2145 SyNergy – ID 390857198 and EXC 390939984, CIBSS - ID 390939984), through SFB 1160, SFB/TRR 167, SFB 1425, GRK 2606, FOR 2879, SFB TRR 274 and under the grants LI-2534/2-1, LI-2534/5-1 and HO-2783/9-1.

Author Contributions

SR performed most experiments, analyzed data and contributed to writing the manuscript; JC, VS, ST, GH, TL, JDB, DC, JZ, AR, OG, YA, JY, MSL, and MR performed experiments and analyzed data; DB, SZ, OG, MD and VH contributed critical material and techniques for this study; DB, OG and VH contributed critical input to study design and manuscript writing; AL initiated and coordinated the study, analyzed data and wrote the manuscript.

Declaration of Interests

All authors declare to have no competing interests

Figure legends

Figure 1. Post-stroke induction of FasL$^+$ myeloid cells by blood factors results in bystander T cell death. (**A**) Parabionts underwent stroke or sham surgery and were euthanized 18h after surgical procedure for flow cytometry quantification of CD45$^+$CD3$^+$ splenic T cells of both the operated and non-operated parabionts (n=10 per group; H-test). (**B**) Whole splenocytes or purified T cells were isolated from naïve animals and then incubated with serum from stroke-or sham-operated mice for 12h. Absolute cell count quantification of T cells was performed by flow cytometry (n=6-7 per group; U-test), results are normalized to the mean of the respective sham serum treated group. (**C**) Schematic of co-culture experimental paradigm. BMDMs were stimulated with stroke or sham serum for 10min; then, BMDMs were washed and the medium exchanged, preventing that T cells get in direct contact with the mouse serum (see methods section for more details). Either BMDM supernatant was used to stimulated T cells or T cells were directly added to BMDMs enabling cell-cell contact. (**D**) Only co-culture of stimulated BMDMs and T cells that allowed cell-cell contact resulted in T cell death (n=6 per group, H-test). (**E**) t-SNE plots of flow cytometric data from whole murine spleen 18h after sham or stroke surgery color-coded by the epitope markers for T cells (CD4$^+$ Thelper and CD8$^+$ Tcytotoxic), CD19$^+$ B cells and CD11b$^+$ monocytes (left panels) and FasL expression in leukocytes (right panels). Comparison of sham and stroke conditions reveals a population of tissue injury-induced myeloid cells (TIM) expressing high amounts of FasL (n=8 mice per group; 3,000 CD45$^+$ cells per mouse). (**F**) Flow cytometry analysis of splenic CD3$^+$ T cells in WT mice treated with isotype control (IgG) or FasL-specific neutralizing antibodies and sacrificed for analysis 18h after stroke or sham surgery (n= 7 per group; U test). (**G**) T cell death was analyzed by PI uptake in a co-culture approach of WT or Fas-deficient (*Fas*^{lpr}) T cells with WT BMDMs enabling cell-cell contact as depicted in (C). PI uptake was quantified by live cell imaging and is presented as percentage of the respective sham group (n=6 per group; U-test per genotype). (**H**) *Rag-1*$^{-/-}$ mice received adoptive transfer of WT or *Fas*^{lpr} T cells. 4 weeks later these mice underwent sham or stroke surgery and splenic T cell counts were analyzed 18h later (n= 6-7 per group; U-test). Please also see Figures S1 and S2 for additional information.

Figure 2. Post-injury IL-1β secretion mediates the T cell cytotoxic FasL+ myeloid cell population. (**A**) Multiplex ELISA for cytokines and chemokines in serum of sham- or stroke-operated mice (normalized to sham group, n= 8 per group, U-test). (**B**) BMDMs were stimulated with rIL-1β in increasing doses. T cells were added after medium change (allowing no direct contact of T cells to rIL-1β), FasL expression and T cell death was analyzed 180min later. rIL-1β dose-dependently increased the ratio of FasL$^+$ monocytes as well as increased T cell death (n= 6 per group, H-test). (**C**) Flow cytometry analysis of FasL-expressing splenic monocytes in WT mice treated with isotype control (IgG) or IL-1β-specific antibodies after sham or stroke surgery. Grey shaded boxes display the mean fluorescence intensity (MFI) for FasL in the respective sham and stroke groups (n=8 per group). (**D**) Mice received either neutralizing anti-IL-1β antibodies or control antibodies 1h prior to and 1h after sham or stroke surgery and 18h later splenic T cells counts were quantified (normalized to sham group, n=6-7 per group, U-test). (**E, F**) WT mice received rIL-1β (100 or 1000 ng) as a single i.p. injection and were sacrificed 6h later. We observed a dose-dependent increase in (E) T cell death and (F) associated monocytic FasL expression in the spleen (n= 4-6 per group; H-test).

Figure 3. Myeloid FasL expression and bystander death of T cells is inflammasome dependent. (**A**) Representative immunoblot micrograph of the different cleavage forms of caspase-1 (Casp1) in splenocyte lysates 12h after stroke or sham surgery (representative for 5 individual experiments). (**B**) Primary monocytes from human blood were isolated and stimulated with either healthy control or stroke patient serum (Pam3CSK4 for priming, Nigericin as positive control). Representative immunoblot photographs of the different cleavage forms of caspase-1 and IL-1β detected in stimulated human monocyte lysates (Lys) and culture supernatants (Sup). Quantification in Suppl. Fig. 3B (Image

is representative for 3 independent experiments). (**C**) The frequency of myeloid cells ($CD45^+CD11b^+$) containing ASC specks was analyzed by flow cytometry imaging of spleens from ASC-citrine reporter mice at 6h after stroke or sham surgery. Cell count analysis for monocytes (600 monocytes in total, 100 randomly selected cells per mouse, 3 mice per condition, U-test) with the indicated number of ASC^+ specks. (**D**) Splenic T cell counts were analyzed in caspase-1 deficient (*Casp1*$^{-/-}$) and wildtype (WT) mice 18h after sham and stroke surgery (n=7 per group; U-test), revealing significantly improved T cell survival in *Casp1*$^{-/-}$ mice. (**E**) Quantification of splenic T cell counts in myeloid cell-specific ASC-deficient (*Lyz2-cre x Asc*$^{fl/fl}$ mice) and WT mice 18h after stroke or sham surgery (n=7 per group; U-test). For additional information please also see Figure S3.

Figure 4. Sensing of cell-free DNA by the AIM2 inflammasome initiates a pathway of bystander cell death in T cells. (A) Double strand (ds) DNA concentrations were measured in mouse serum 6h after stroke or sham surgery (n=6-8 per group; U-test). (**B**) dsDNA concentrations were analyzed in serum of stroke patients in comparison to age-matched healthy control patients (n=20 per group; U-test). (**C**) Plasma of hrDNase or control-treated mice was collected 18h after stroke or sham surgery. Acquisiton of DNA concentrations revealed a significant decrease of dsDNA in hrDNase-treated mice after stroke (n=6 per group; H-test). (**D-F**) Cell-free dsDNA was therapeutically degraded by *i.p.* administration of hrDNase after stroke. hrDNase treatment significantly reduced monocyte inflammasome activation as measured by FAM FLICA flow cytometry analysis (D), reduced FasL expression on monocytes (E) and rescued splenic T cell survival (F) (n=5-7 per group; U-test). (**G, H**) Correspondingly, comparison of WT and AIM2-deficient (*Aim2*$^{-/-}$) mice revealed a similar pattern of reduced inflammasome activation in monocytes (G) and improved T cell survival (H) in spleens of *Aim2*$^{-/-}$ mice after stroke (n=5-13 per group; U-test). (**I**) BMDMs were stimulated with stroke or sham serum, the serum was removed and $eGFP^+$ T cells were added for subsequent live imaging of $eGFP^+$ T cell survival in co-culture with WT or *Aim2*$^{-/-}$ BMDMs. Results are shown as T cell death rate for T cells in the stroke-serum normalized to sham serum-treated BMDMs culture conditions (n= 4 per group, 2-way ANOVA). Please also see Figures S4 and S5 for additional information.

Figure 5. Inflammasome-dependent T cell death predisposes to infections in stroke patients and exacerbates bacterial infections in a stroke model. (**A**) Schematic description of patient characteristics and sequential analysis of acute mediators at d0 and d1 and subacute infections (d2-d7) after stroke. (**B**) Left: dsDNA and IL-1β concentrations upon hospital admission were significantly associated in univariate linear regression analysis (R^2=0.052). Right: IL-1β concentrations upon admission were negatively associated with lymphocyte counts at d1 in a multivariable linear regression model adjusting for age and sex (R^2=0.16). The linear fit (dashed line) and 95% confidence intervals are shown in color. (**C**) IL-1β concentrations were significantly increased (left) and lymphocyte counts significantly decreased (right) in patients with subsequent infections (n=50) during the subacute phase (d2-7) after stroke compared to patients without infections (n=124). Multivariable linear regression model adjusting for age and sex. (**D**) Path diagram of the mediation model including all 174 patients showing full mediation of IL-1β effects on infection via reduction of blood lymphocyte counts. C and c' indicate beta values for the direct effect without or with inclusion of lymphocyte counts in the model, respectively. (**E**) Splenic T cells of VX765 (Caspaspe-1 inhibitor) or control-treated WT mice were analyzed by flow cytometry 18h after stroke or sham surgery (n=5 per group; U-test). (**F, G**) Mice received VX765 or control treatment and underwent stroke or sham surgery, 12h after the surgery they were intranasally inoculated with 10^6 CFU of *S. pneumoniae* or $2x10^5$ *K. pneumoniae*, 14h later the CFU burden in the respiratory tract (*S. pneumoniae*: trachea; *K. pneumoniae*: lung) was determined. (**H**) Schematic overview of the proposed mechanism.

References

Ayasoufi, K., Pfaller, C.K., Evgin, L., Khadka, R.H., Tritz, Z.P., Goddery, E.N., Fain, C.E., Yokanovich, L.T., Himes, B.T., Jin, F.*, et al.* (2020). Brain cancer induces systemic immunosuppression through release of non-steroid soluble mediators. Brain.

Barlow, Y. (1994). T lymphocytes and immunosuppression in the burned patient: a review. Burns *20*, 487-490.

Baron, R.M., and Kenny, D.A. (1986). The moderator-mediator variable distinction in social psychological research: conceptual, strategic, and statistical considerations. J Pers Soc Psychol *51*, 1173-1182.

Bohannon, J., Cui, W., Cox, R., Przkora, R., Sherwood, E., and Toliver-Kinsky, T. (2008). Prophylactic treatment with fms-like tyrosine kinase-3 ligand after burn injury enhances global immune responses to infection. J Immunol *180*, 3038-3048.

Bouillet, P., and O'Reilly, L.A. (2009). CD95, BIM and T cell homeostasis. Nat Rev Immunol *9*, 514-519.

Brinkman, W., Herbert, M.A., O'Brien, S., Filardo, G., Prince, S., Dewey, T., Magee, M., Ryan, W., and Mack, M. (2014). Preoperative beta-blocker use in coronary artery bypass grafting surgery: national database analysis. JAMA Intern Med *174*, 1320-1327.

Chamorro, A., Meisel, A., Planas, A.M., Urra, X., van de Beek, D., and Veltkamp, R. (2012). The immunology of acute stroke. Nat Rev Neurol *8*, 401-410.

D'Avignon, L.C., Hogan, B.K., Murray, C.K., Loo, F.L., Hospenthal, D.R., Cancio, L.C., Kim, S.H., Renz, E.M., Barillo, D., Holcomb, J.B.*, et al.* (2010). Contribution of bacterial and viral infections to attributable mortality in patients with severe burns: an autopsy series. Burns *36*, 773-779.

Denes, A., Coutts, G., Lenart, N., Cruickshank, S.M., Pelegrin, P., Skinner, J., Rothwell, N., Allan, S.M., and Brough, D. (2015). AIM2 and NLRC4 inflammasomes contribute with ASC to acute brain injury independently of NLRP3. Proc Natl Acad Sci U S A *112*, 4050-4055.

Dockrell, D.H., Badley, A.D., Villacian, J.S., Heppelmann, C.J., Algeciras, A., Ziesmer, S., Yagita, H., Lynch, D.H., Roche, P.C., Leibson, P.J., and Paya, C.V. (1998). The expression of Fas Ligand by macrophages and its upregulation by human immunodeficiency virus infection. J Clin Invest *101*, 2394-2405.

Drexler, S.K., Bonsignore, L., Masin, M., Tardivel, A., Jackstadt, R., Hermeking, H., Schneider, P., Gross, O., Tschopp, J., and Yazdi, A.S. (2012). Tissue-specific opposing functions of the inflammasome adaptor ASC in the regulation of epithelial skin carcinogenesis. Proc Natl Acad Sci U S A *109*, 18384-18389.

Fas, S.C., Fritzsching, B., Suri-Payer, E., and Krammer, P.H. (2006). Death receptor signaling and its function in the immune system. Curr Dir Autoimmun *9*, 1-17.

Finnerty, C.C., Herndon, D.N., Przkora, R., Pereira, C.T., Oliveira, H.M., Queiroz, D.M., Rocha, A.M., and Jeschke, M.G. (2006). Cytokine expression profile over time in severely burned pediatric patients. Shock *26*, 13-19.

Fuchs, H.J., Borowitz, D.S., Christiansen, D.H., Morris, E.M., Nash, M.L., Ramsey, B.W., Rosenstein, B.J., Smith, A.L., and Wohl, M.E. (1994). Effect of aerosolized recombinant human DNase on exacerbations of respiratory symptoms and on pulmonary function in patients with cystic fibrosis. The Pulmozyme Study Group. N Engl J Med *331*, 637-642.

Girardot, T., Rimmele, T., Venet, F., and Monneret, G. (2017). Apoptosis-induced lymphopenia in sepsis and other severe injuries. Apoptosis *22*, 295-305.

Guo, H., Callaway, J.B., and Ting, J.P. (2015). Inflammasomes: mechanism of action, role in disease, and therapeutics. Nat Med *21*, 677-687.

Hornung, V., Ablasser, A., Charrel-Dennis, M., Bauernfeind, F., Horvath, G., Caffrey, D.R., Latz, E., and Fitzgerald, K.A. (2009). AIM2 recognizes cytosolic dsDNA and forms a caspase-1-activating inflammasome with ASC. Nature *458*, 514-518.

Hotchkiss, R.S., Monneret, G., and Payen, D. (2013). Sepsis-induced immunosuppression: from cellular dysfunctions to immunotherapy. Nat Rev Immunol *13*, 862-874.

Huang, H.W., Tang, J.L., Han, X.H., Peng, Y.P., and Qiu, Y.H. (2013). Lymphocyte-derived catecholamines induce a shift of Th1/Th2 balance toward Th2 polarization. Neuroimmunomodulation *20*, 1-8.

Hundeshagen, G., Cui, W., Musgrove, L., Cherry, A., Lee, S.J., Cox, R.A., and Toliver-Kinsky, T. (2018). Fms-Like Tyrosine Kinase-3 Ligand Attenuates Local and Systemic Infection in a Model of Post-Burn Pneumonia. Shock *49*, 721-727.

Kilkenny, C., Browne, W.J., Cuthill, I.C., Emerson, M., and Altman, D.G. (2010). Improving bioscience research reporting: the ARRIVE guidelines for reporting animal research. PLoS Biol *8*, e1000412.

Kimmelman, J., Mogil, J.S., and Dirnagl, U. (2014). Distinguishing between exploratory and confirmatory preclinical research will improve translation. PLoS Biol *12*, e1001863.

Krammer, P.H., Arnold, R., and Lavrik, I.N. (2007). Life and death in peripheral T cells. Nat Rev Immunol *7*, 532-542.

Krammer, P.H., Behrmann, I., Daniel, P., Dhein, J., and Debatin, K.M. (1994). Regulation of apoptosis in the immune system. Curr Opin Immunol *6*, 279-289.

Kroemer, G., Galluzzi, L., Kepp, O., and Zitvogel, L. (2013). Immunogenic cell death in cancer therapy. Annu Rev Immunol *31*, 51-72.

Lambertsen, K.L., Biber, K., and Finsen, B. (2012). Inflammatory cytokines in experimental and human stroke. J Cereb Blood Flow Metab *32*, 1677-1698.
Latz, E., Xiao, T.S., and Stutz, A. (2013). Activation and regulation of the inflammasomes. Nat Rev Immunol *13*, 397-411.
Li, T., Pang, S., Yu, Y., Wu, X., Guo, J., and Zhang, S. (2013). Proliferation of parenchymal microglia is the main source of microgliosis after ischaemic stroke. Brain *136*, 3578-3588.
Li-Weber, M., and Krammer, P.H. (2003). Function and regulation of the CD95 (APO-1/Fas) ligand in the immune system. Semin Immunol *15*, 145-157.
Liesz, A., Dalpke, A., Mracsko, E., Antoine, D.J., Roth, S., Zhou, W., Yang, H., Na, S.Y., Akhisaroglu, M., Fleming, T.*, et al.* (2015). DAMP signaling is a key pathway inducing immune modulation after brain injury. J Neurosci *35*, 583-598.
Liesz, A., Hagmann, S., Zschoche, C., Adamek, J., Zhou, W., Sun, L., Hug, A., Zorn, M., Dalpke, A., Nawroth, P., and Veltkamp, R. (2009a). The spectrum of systemic immune alterations after murine focal ischemia: immunodepression versus immunomodulation. Stroke *40*, 2849-2858.
Liesz, A., Ruger, H., Purrucker, J., Zorn, M., Dalpke, A., Mohlenbruch, M., Englert, S., Nawroth, P.P., and Veltkamp, R. (2013). Stress mediators and immune dysfunction in patients with acute cerebrovascular diseases. PLoS One *8*, e74839.
Liesz, A., Suri-Payer, E., Veltkamp, C., Doerr, H., Sommer, C., Rivest, S., Giese, T., and Veltkamp, R. (2009b). Regulatory T cells are key cerebroprotective immunomodulators in acute experimental stroke. Nat Med *15*, 192-199.
Llovera, G., Hofmann, K., Roth, S., Salas-Perdomo, A., Ferrer-Ferrer, M., Perego, C., Zanier, E.R., Mamrak, U., Rex, A., Party, H.*, et al.* (2015). Results of a preclinical randomized controlled multicenter trial (pRCT): Anti-CD49d treatment for acute brain ischemia. Sci Transl Med *7*, 299ra121.
Llovera, G., and Liesz, A. (2016). The next step in translational research: lessons learned from the first preclinical randomized controlled trial. J Neurochem *139 Suppl 2*, 271-279.
Loftus, T.J., Efron, P.A., Moldawer, L.L., and Mohr, A.M. (2016). beta-Blockade use for Traumatic Injuries and Immunomodulation: A Review of Proposed Mechanisms and Clinical Evidence. Shock *46*, 341-351.
Lord, J.M., Midwinter, M.J., Chen, Y.F., Belli, A., Brohi, K., Kovacs, E.J., Koenderman, L., Kubes, P., and Lilford, R.J. (2014). The systemic immune response to trauma: an overview of pathophysiology and treatment. Lancet *384*, 1455-1465.
Meisel, C., and Meisel, A. (2011). Suppressing immunosuppression after stroke. N Engl J Med *365*, 2134-2136.
Meisel, C., Schwab, J.M., Prass, K., Meisel, A., and Dirnagl, U. (2005). Central nervous system injury-induced immune deficiency syndrome. Nat Rev Neurosci *6*, 775-786.
Mracsko, E., Liesz, A., Karcher, S., Zorn, M., Bari, F., and Veltkamp, R. (2014). Differential effects of sympathetic nervous system and hypothalamic-pituitary-adrenal axis on systemic immune cells after severe experimental stroke. Brain Behav Immun *41*, 200-209.
Norbury, W.B., Herndon, D.N., Branski, L.K., Chinkes, D.L., and Jeschke, M.G. (2008). Urinary cortisol and catecholamine excretion after burn injury in children. J Clin Endocrinol Metab *93*, 1270-1275.
Ormstad, H., Aass, H.C., Lund-Sorensen, N., Amthor, K.F., and Sandvik, L. (2011). Serum levels of cytokines and C-reactive protein in acute ischemic stroke patients, and their relationship to stroke lateralization, type, and infarct volume. J Neurol *258*, 677-685.
Panahi, M., Papanikolaou, A., Torabi, A., Zhang, J.G., Khan, H., Vazir, A., Hasham, M.G., Cleland, J.G.F., Rosenthal, N.A., Harding, S.E., and Sattler, S. (2018). Immunomodulatory interventions in myocardial infarction and heart failure: a systematic review of clinical trials and meta-analysis of IL-1 inhibition. Cardiovasc Res *114*, 1445-1461.
Poh, L., Kang, S.W., Baik, S.H., Ng, G.Y.Q., She, D.T., Balaganapathy, P., Dheen, S.T., Magnus, T., Gelderblom, M., Sobey, C.G.*, et al.* (2019). Evidence that NLRC4 inflammasome mediates apoptotic and pyroptotic microglial death following ischemic stroke. Brain Behav Immun *75*, 34-47.
Prass, K., Meisel, C., Hoflich, C., Braun, J., Halle, E., Wolf, T., Ruscher, K., Victorov, I.V., Priller, J., Dirnagl, U.*, et al.* (2003). Stroke-induced immunodeficiency promotes spontaneous bacterial infections and is mediated by sympathetic activation reversal by poststroke T helper cell type 1-like immunostimulation. J Exp Med *198*, 725-736.
Pruss, H., Tedeschi, A., Thiriot, A., Lynch, L., Loughhead, S.M., Stutte, S., Mazo, I.B., Kopp, M.A., Brommer, B., Blex, C.*, et al.* (2017). Spinal cord injury-induced immunodeficiency is mediated by a sympathetic-neuroendocrine adrenal reflex. Nat Neurosci *20*, 1549-1559.
Ridker, P.M., Everett, B.M., Thuren, T., MacFadyen, J.G., Chang, W.H., Ballantyne, C., Fonseca, F., Nicolau, J., Koenig, W., Anker, S.D.*, et al.* (2017). Antiinflammatory Therapy with Canakinumab for Atherosclerotic Disease. N Engl J Med *377*, 1119-1131.
Rubio, I., Osuchowski, M.F., Shankar-Hari, M., Skirecki, T., Winkler, M.S., Lachmann, G., La Rosee, P., Monneret, G., Venet, F., Bauer, M.*, et al.* (2019). Current gaps in sepsis immunology: new opportunities for translational research. Lancet Infect Dis *19*, e422-e436.

Singh, V., Sadler, R., Heindl, S., Llovera, G., Roth, S., Benakis, C., and Liesz, A. (2018). The gut microbiome primes a cerebroprotective immune response after stroke. J Cereb Blood Flow Metab *38*, 1293-1298.
Strasser, A., Jost, P.J., and Nagata, S. (2009). The many roles of FAS receptor signaling in the immune system. Immunity *30*, 180-192.
Tettelin, H., Nelson, K.E., Paulsen, I.T., Eisen, J.A., Read, T.D., Peterson, S., Heidelberg, J., DeBoy, R.T., Haft, D.H., Dodson, R.J.*, et al.* (2001). Complete genome sequence of a virulent isolate of Streptococcus pneumoniae. Science *293*, 498-506.
Toliver-Kinsky, T.E., Cui, W., Murphey, E.D., Lin, C., and Sherwood, E.R. (2005). Enhancement of dendritic cell production by fms-like tyrosine kinase-3 ligand increases the resistance of mice to a burn wound infection. J Immunol *174*, 404-410.
Tzeng, T.C., Schattgen, S., Monks, B., Wang, D., Cerny, A., Latz, E., Fitzgerald, K., and Golenbock, D.T. (2016). A Fluorescent Reporter Mouse for Inflammasome Assembly Demonstrates an Important Role for Cell-Bound and Free ASC Specks during In Vivo Infection. Cell Rep *16*, 571-582.
Vanderweele, T.J., and Vansteelandt, S. (2010). Odds ratios for mediation analysis for a dichotomous outcome. Am J Epidemiol *172*, 1339-1348.
Westendorp, W.F., Vermeij, J.D., Brouwer, M.C., Roos, Y.B., Nederkoorn, P.J., van de Beek, D., and Investigators, P. (2016). Pre-Stroke Use of Beta-Blockers Does Not Lower Post-Stroke Infection Rate: An Exploratory Analysis of the Preventive Antibiotics in Stroke Study. Cerebrovasc Dis *42*, 506-511.
Woiciechowsky, C., Asadullah, K., Nestler, D., Eberhardt, B., Platzer, C., Schoning, B., Glockner, F., Lanksch, W.R., Volk, H.D., and Docke, W.D. (1998). Sympathetic activation triggers systemic interleukin-10 release in immunodepression induced by brain injury. Nat Med *4*, 808-813.
Wright, D.E., Wagers, A.J., Gulati, A.P., Johnson, F.L., and Weissman, I.L. (2001). Physiological migration of hematopoietic stem and progenitor cells. Science *294*, 1933-1936.
Wu, T., Xu, F., Su, C., Li, H., Lv, N., Liu, Y., Gao, Y., Lan, Y., and Li, J. (2020). Alterations in the Gut Microbiome and Cecal Metabolome During Klebsiella pneumoniae-Induced Pneumosepsis. Front Immunol *11*, 1331.

STAR methods

Resources availability

Lead contact

Further information and requests for resources and reagents should be directed to and will be fulfilled by the lead contact, Arthur Liesz, (Arthur.Liesz@med.uni-muenchen.de).

Material availability

This study did not generate new unique reagents.

Data and Code availability

All original raw data of flow cytometric analyses are publicly available in the zenodo open data repository under the DOI: 10.5281/zenodo.4311586.

Experimental model and subject details

Clinical patient populations.

Stroke patients: Ischemic stroke patients were recruited within 24 hours of symptom onset through the emergency department at the LMU University Hospital Munich (Germany), a tertiary level hospital. All patients had a final diagnosis of ischemic stroke as defined by 1) an acute focal neurological deficit in combination with a diffusion weighted imaging-positive lesion on magnetic resonance imaging, or 2) a new lesion on a delayed CT scan.

For analysis of blood dsDNA concentrations (Figure 4B), we included 20 stroke patients with infarct volumes >50ml and 20 age-matched control patients which were recruited in the neurological outpatient clinic.

Patient characteristics for analysis shown in Figure 4B:

	Stroke (n=20)	Control (n=20)
Age	74 (10)	74 (10)
Sex (female)	20 % (4)	20 % (4)
Infarct volume	126ml (101ml)	N/A
Time after stroke onset	4.0 h (2.3h)	N/A

(shown as Mean (SD))

For analysis of secondary infections (Figure 5A-D), 174 stroke patients were included. Secondary infections were defined as clinically diagnosed by the treating physician and additionally confirmed by either blood C-reactive protein (CRP) concentration >30 mg/l and/or radiographic (chest X-ray or CT) confirmation of pneumonia. The study was approved by the local ethics committee and was conducted in accordance with the Declaration of Helsinki as well as institutional guidelines. Written and informed consent was obtained from all patients.

Patient characteristics for analyses shown in Figure 5A-D:

	No infection (N=124)	Infection (N=50)	P
Age, median (IQR) [years]	76 (66-82)	80 (71-85)	0.012
Female, % (n)	44 (55)	54 (27)	0.314
Baseline NIHSS score, median (IQR)	3 (1-8)	15 (7-21)	<0.001
Infarct volume, median (IQR) [ml]	2 (0-10)	29 (5-107)	<0.001

Thermal injury patients: Patients (all male) with severe burn injury encompassing more than 40% of total body surface area (TBSA) were recruited through BG Trauma Center Ludwigshafen (Germany). TBSA was assessed on admission by the attending burn surgeon using Lund-Browder charts and serum samples were collected at 24 hours post burn. Age- and sex-matched control patients were recruited in the trauma center outpatient clinic. The study was approved by the local ethics committee and was conducted in accordance with the Declaration of Helsinki as well as institutional guidelines. Written and informed consent was obtained from all patients.

	Burn	Control
Age	58 (16)	54 (13)
TBSA	57 % (6%)	N/A

(shown as Mean (SD))

Animal experiments.

All animal experiments were performed in accordance with the guidelines for the use of experimental animals and were approved by the respective governmental committees (Regierungspraesidium Oberbayern, the Rhineland Palatinate Landesuntersuchungsamt Koblenz, and the Ethics Committee of Lanzhou University). Wild type C57BL6/J mice, *Rag-1*$^{-/-}$ (NOD.129S7(B6)-*Rag-1*$^{tm1Mom/J}$), *Casp1*$^{-/-}$(B6N.129S2-*Casp1*$^{<tm1Flv>}$/J) were bred and housed at the animal core facility of the Center for Stroke and Dementia Research (Munich, Germany). The ASC-Citrine reporter mice (B6. Cg-Gt(ROSA)26Sor$^{tm1.1(CAG-Pycard/mCitrine*,-CD2)Dtg}$/J) and *Fas*^{lpr} (MRL/MpJ-Fas^{lpr}/J) were obtained from Jackson Laboratory (Bar Harbor, USA). *Aim2*$^{-/-}$ mice (Aim2$^{<tm1.2Arte>}$) where bred at the Institute for Innate

Immunity, University Bonn (Germany). *Pycard*$^{-/-}$ mice (B6.129S5-Pycard^{tm1Vmd}) were bred at the Gene Center of the LMU University Munich (Germany). Myeloid-specific ASC-deficient mice (*Lyz2-cre* x *Pycard*$^{fl/fl}$)(Drexler et al., 2012) mice were bred at Charles River (Calco, Italy). Cx3Cr1$^{GFP/+}$ mice were purchased from Jackson Laboratory (Bar Harbor, USA) and bred at the animal core facility of Lanzhou University. All mice were housed with free access to food and water at a 12h dark-light cycle.

For this exploratory study, animal numbers were estimated based on previous results from the transient ischemia-reperfusion stroke model on extent and variability of T cell death after stroke. Data was excluded from all mice that died during surgery. Detailed exclusion criteria are described below. Animals were randomly assigned to treatment groups and all analyses were performed by investigators blinded to group allocation. All animal experiments were performed and reported in accordance with the ARRIVE guidelines (Kilkenny et al., 2010).

Method details

Transient ischemia-reperfusion stroke model. Mice were anaesthetized with isoflurane delivered in a mixture of 30% O_2 and 70% N_2O. An incision was made between the ear and the eye in order to expose the temporal bone. Mice were placed in supine position, and a laser Doppler probe was affixed to the skull above the middle cerebral artery (MCA) territory. The common carotid artery and left external carotid artery were exposed via midline incision and further isolated and ligated. A 2-mm silicon-coated filament (Doccol) was inserted into the internal carotid artery, advanced gently to the MCA until resistance was felt, and occlusion was confirmed by a corresponding decrease in blood flow (i.e., a decrease in the laser Doppler flow signal by ≥ 80 %. After 60 minutes of occlusion, the animals were re-anesthetized, and the filament was removed. After recovery, the mice were kept in their home cage with *ad libitum* access to water and food. Sham-operated mice received the same surgical procedure, but the filament was removed in lieu of being advanced to the MCA. Body temperature was maintained at 37 °C throughout surgery in all mice via feedback-controlled heating pad. The overall mortality rate of animals subjected to MCA occlusion was approximately 20 %. All animals in the sham group survived the procedure. Exclusion criteria: 1. Insufficient MCA occlusion (a reduction in blood flow to >20% of the baseline value). 2. Death during the surgery. 3. Lack of brain ischemia as quantified post-mortem by histological analysis.

Germfree (GF) mouse handling. All surgeries, housing and post-operative animal handling were performed under sterile conditions as previously described (Singh et al., 2018). In brief, stroke and sham surgeries have been performed under sterile conditions in a microbiological safety cabinet, animals received sterilized water and irradiated food and animals were kept in sterile gnotocage mini-isolators. All surgical procedures and post-surgical care were otherwise performed as stated above.

Experimental thermal trauma model. As previously described(Hundeshagen et al., 2018), male C57Bl/6J mice (Charles River, Freiburg, Germany), aged 7-8 weeks, received a 35 % total body surface area (TBSA) full thickness scald burn to the back through 10 seconds immersion in 98 °C water under deep anesthesia with 2 % isoflurane and analgesia with 0.1 mg kg-1 buprenorphine. Immediately after burn injury, the mice were resuscitated with 2 ml of lactated Ringer's solution (via i.p. injection as previously described(Bohannon et al., 2008; Hundeshagen et al., 2018; Toliver-Kinsky et al., 2005). Animals in the sham burn group were subjected to identical treatment except for water temperature during immersion being 36 °C. Following burn injury or sham burn, mice were singly housed at room temperature (21°C).

Parabiosis. Parabiosis experiments were performed at the Gansu Key Laboratory of Biomonitoring and Bioremediation for Environmental Pollution in Lanzhou, China. Pairs of weight-matched wild type C57Bl6/J and heterozygous $Cx3Cr1^{GFP/+}$ mice were subjected to parabiotic surgery (Li et al., 2013; Wright et al., 2001). $Cx3Cr1^{GFP/+}$ mice were used as the non-operated parabiont in all parabiont pairs in order to confirm successful chimerism between both parabionts by flow cytometric analysis of

Post-injury T cell death

GFP^+ cell frequency in both animals at the end of experiment (Suppl. Fig. 2B). Animals were anesthetized by intraperitoneal injection of 20 mg/ml ketamine and 2 mg/ml xylazine. The flanks were shaved and sterilized. An incision from behind the ear to the hip was made on the opposing sides of two mice. Opposing posterior muscles were joined with a 5-0 suture. The scapular region was conjoined then dorsal and ventral skin edges were sutured with a 4-0 suture. Mice were kept at 37˚C in a recovery box until completely recovered from anesthesia. During the first 7 days after surgery, Tylenol is mixed in the food for analgesic purposes. Food and water were provided *ad libitum*. The optimized procedure had a survival rate of ≥ 75 %.

Intranasal bacterial infection. Pneumococcal infection experiments were performed at the Helmholtz Centre for Infection Research (HZI) in Braunschweig, Germany. Mice were anesthetized with isoflurane delivered in a mixture of 30% O_2 and 70% N_2O. The inoculum (10^6 CFU of TIGR4, a serotype 4 *S. pneumoniae* strain (Tettelin et al., 2001) or $2x10^5$ CFU of *K.pneumoniae subsp. pneumoniae (*ATCC 43816) *(Wu et al., 2020)* in a total volume of 25µl PBS) was administered with a pipette onto the nostrils of the mice.

Drug administrations.

Anti-IL1β: Mice received two injections of antagonizing anti-IL-1β in sterile saline (clone: B122, InVivoMab, BioXcell, US), 1 hour prior to and 1 hour after surgery. Anti-IL-1β or the corresponding IgG control (Armenian hamster IgG, InVivoMab, BioXcell, US) was injected i.p. at a dose of 4 mg kg^{-1} body weight in a final volume of 200 µl.

Anti-FasL: Mice received two injections of antagonizing anti-FasL in sterile saline (clone: MFL3, InVivoMab, BioXcell, US), 1 hour prior to and 1 hour after surgery. Anti-FasL or the corresponding IgG control (Armenian hamster IgG, InVivoMab, BioXcell, US) was injected i.p. at a dose of 4 mg kg^{-1} body weight in a final volume of 100 µl.

Human recombinant DNase (hrDNase): 1000 U of human recombinant DNase (Roche, Switzerland) dissolved in incubation 1x buffer (40 mM Tris-HCl, 10 mM NaCl, 6 mM $MgCl_2$, 1 mM $CaCl_2$, pH 7.9, diluted in PBS, Roche) was injected i.v. in the tail vein 1 hour after surgery in a final volume of 100 µl. The control group was administered vehicle injections at the same volume, route, and timing as experimental animals.

Caspase-1 inhibitor (VX-765): The caspase-1 inhibitor VX-765 in DMSO dissolved in PBS (Belnacasan, Invivogen, US) was injected i.p. 1 hour prior to surgery at a dose of 100 mg kg^{-1} body weight at a final volume of 300 µl. The control group was administered vehicle injections at the same volume, route, and timing as experimental animals.

Caspase-8 inhibitor (Z-IETD-FMK) & Caspase-9 inhibitor (Z-LEHD-FMK): The apoptosis inhibitors Z-IETD-FMK and Z-LEHD-FMK (R&D systems, US) in DMSO dissolved in PBS and injected *i.p.* 30 minutes after surgery. Z-LEHD-FMK was injected at a dose of 0.8 µM kg^{-1} body weight at a final

volume of 200 µl. Z-IETD-FMK was injected at a dose of 0.8 mg kg^{-1} body weight at a final volume of 100 µl. The control groups were administered vehicle injections at the same volume, route, and timing as experimental animals.

Selective Beta2-adrenoreceptor inhibitor (ICI-118,551): The β2-adrenoreceptor inhibitor ICI118,551 (Sigma, Germany) was dissolved in PBS and administered 1 hour prior to and 1 hour after surgery at a dose of 4 mg kg^{-1} body weight at a final volume of 200 µl. The control group was administered vehicle injections at the same volume, route, and timing as experimental animals.

Murine recombinant IL-1β: Recombinant IL-1β (401-ML, R&D systems, US) was diluted in sterile PBS and administered intraperitoneally at a dose of 100 or 1000 ng per mouse in a total volume of 100 µl. The control group was administered vehicle injections at the same volume, route and timing as experimental animals.

Adoptive T cell transfer in *Rag-1*$^{-/-}$ recipient mice. Donor animals (C57BL6/J, *Fas*^{lpr}) were euthanized and spleens were collected in Dulbecco's Modified Eagle Medium (DMEM+GlutaMax). Spleens were homogenized and filtered through 40 µm cell strainers. T cells were enriched using a negative selection kit for $CD3^+$ T cells (*MagniSort*, Thermo Fisher). After washing and quantification, cells were injected i.p. into *Rag-1*$^{-/-}$ recipient mice (10^7 $CD3^+$ T cells per mouse) in a total volume of 200 µl saline. Mice were maintained for 4 weeks in order to establish a functional T cell niche, and then assigned to the surgery groups.

Organ and tissue processing. Mice were deeply anaesthetized with ketamine (120 mg/kg) and xylazine (16 mg/kg) and blood was drawn via cardiac puncture in 50mM EDTA (Sigma-Aldrich). Plasma was isolated by centrifugation at 3,000 g for 10 minutes and stored at -80 °C until further use. The blood pellet was resuspended in DMEM and erythrocytes were lysed using isotonic ammonium chloride buffer. Immediately following cardiac puncture, mice were transcardially perfused with normal saline for dissection of bone marrow and spleen. Spleen and bone marrow were transferred to tubes containing Hank's balanced salt solution (HBSS), homogenized and filtered through 40 µm cell strainers to obtain single cell suspensions. Homogenized spleens were subjected to erythrolysis using isotonic ammonium chloride buffer.

Bacterial culture and CFU counts. *S. pneumoniae* TIGR4, an encapsulated strain of serotype 4, was grown overnight on Columbia blood agar plates (37°C, 5%CO_2), single colonies were cultured in Todd-Hewitt broth with 1% yeast extract to mid-logarithmic phase (OD_{600nm}: 0.35), washed, and diluted in sterile PBS to the desired concentration. *Klebsiella pneumoniae subsp. pneumoniae* was grown in Mueller Hinton broth to mid-logarithmic growth phase (OD_{600nm}: 0.7), washed and diluted in PBS. 14h post bacterial infection, mice were euthanized, tracheas and lungs were aseptically removed and mechanically homogenized in PBS. Serial dilutions of lung and tracheal tissue homogenates were plated onto blood agar plates and CFU were determined after 16h of incubation.

Post-injury T cell death

Fluorescence-activated Cell Sorting (FACS) analysis. The anti-mouse antibodies listed below were used for surface marker staining of $CD45^+$ leukocytes, $CD45^+CD11b^+$ monocytes (+ $FasL^+$ expression, FAM FLICA), $CD3^+$ T cells, $CD3^+CD4^+$ T_{helper} cells, $CD3^+CD8^+$ $T_{cytotox}$ cells and $CD19^+$ B cells (see representative gating strategy below). Fc blocking (Anti CD16/CD32, Invitrogen, US) was performed on all samples prior to extracellular antibody staining. All stains were performed according to the manufacturer's protocols. Flow cytometric data was acquired using a BD FACSverse flow cytometer (BD Biosciences, Germany) and analyzed using FlowJo software (Treestar, US). Raw data of all flow cytometry experiments can be found in fcs. data format in the zenodo open data repository under the DOI: 10.5281/zenodo.4311586.

FAM FLICA caspase-1 staining for flow cytometry. To detect the active forms of caspase-1 in blood, spleen, and bone marrow samples, cell suspensions were stained with the fluorescent inhibitor probe FAM-YVAD-FMK (FAM FLICA, BioRad, Germany) for 30 minutes at 37 °C according to the manufacturer's instructions. After washing, the cells were stained for $CD45^+CD3^+$ T cells and $CD45^+CD11b^+$ monocytes. The flow cytometry data was acquired on a BD FACSVerse

Representative gating strategy:

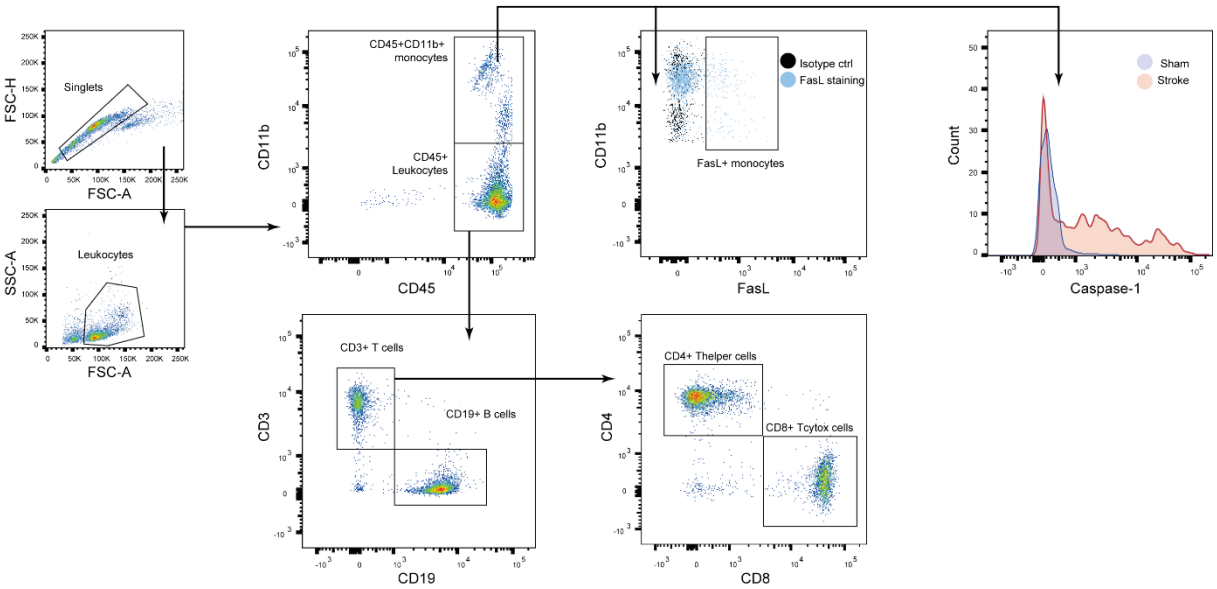

Dimensionality reduction analysis for flow cytometrydata. Flow cytometry data acquired with FACSVerse was pre-analyzed with FlowJo software. To normalize the data, each sample was down-scaled ("DownSample" plugin FlowJo) to 3,000 $CD45^+$ cells per individual mouse. After concatenating the individual samples into a batch, t-distributed stochastic neighboring embedding (t-SNE) analysis was conducted (Parameters: Iterations 550; Perplexity 30; Eta learning rate 200) using the "t-SNE plugin" of the FlowJo software (V10.6).

Flow cytometry imaging of ASC-citrine reporter mice. Spleens from ASC-citrine reporter mice were dissected and single splenocyte suspensions were prepared using a 40µm cell strainer, then

subjected to erythrolysis as described above. Splenocytes were then stained with antibodies against CD45 and CD11b as described above. Cells were resuspended at a concentration of 10^7 cells/ml for flow cytometry imaging using the Flowsight Imaging flow cytometer (Amnis). The results were analyzed using the IDEAS software (Amnis)(Tzeng et al., 2016). For analysis of ASC specks, cells were gated for $CD45^+CD11b^+$ expression. Cells were randomly selected by the software and the presence of ASC specks was manually determined.

FAM FLICA caspase-1 staining on fresh frozen spleen sections. Mice were deeply anesthetized and euthanized as described above. Spleens were immediately removed, embedded in cryotech solution (OCT, tissue-tek, US) and cryosectioned sagittally (20 µm thickness). FAM-YVAD-FMK (FAM FLICA, BioRad, Germany) solution was prepared as indicated in the manufacturer's instruction and sections were incubated for 1 hour at 37 °C. Sections were then washed with PBS, stained with DAPI (1:5,000; Dako, Denmark), and mounted (Aqueous mounting medium, Dako, Denmark). Epifluorescence images were acquired at 20x magnification (Axio Imager 2, Carl Zeiss, Germany).

Whole splenocyte culture. Spleens from naïve wild type mice were dissected and single splenocyte suspensions were prepared using a 40µm cell strainer, then subjected to erythrolysis as described above. Cells were washed three times with PBS, then cell number and viability was assessed using an automated cell counter (BioRad, Germany) and Trypan blue solution (Merck, Germany). Required viability threshold was ≥ 80 %. Cells were cultured (complete RPMI1640, 10 % heat-inactivated fetal bovine serum (FBS), 1 % penicillin/streptomycin, 10 µM β-mercaptoethanol) overnight for 16 hours on a 96 well flat bottom (anti-CD3/CD28 coated) plate at a density of 10^5 cells per 100 µl in a final volume of 200 µl. Cells were then stimulated by 12-hour incubation with serum from either stroke or sham operated mice at a concentration of 25 % total well volume. After the stimulation, cell death and activation status were analyzed by flow cytometry as described above.

Bone Marrow-Derived Macrophages (BMDM) isolation and cell culture. BMDMs were generated from tibia and femur of transcardially perfused mice. After careful isolation and dissection of tibia and femur, bone marrow was flushed out of the bones through a 40 µm strainer using a plunger and 1 ml syringe filled with sterile 1x PBS. Strained bone marrow cells were washed with PBS, and resuspended in DMEM + GlutaMAX-1 (Gibco, US), supplemented with 10 % FBS and 1 % Gentamycin (Thermo Fisher Scientific, US) and counted. 5 x 10^7 cells were plated onto 150 mm culture dishes. Cells were differentiated into BMDMs over the course of 8-10 days. For the first 3 days after isolation, cells were supplemented with 20 % L929 cell-conditioned media (LCM), as a source of M-CSF. Cultures were then maintained at 37°C with 5% CO_2 until ≥ 90% confluency.

T cell isolation and culture. Round-bottom 96-well plates were coated with 100 µl of PBS containing a mixture of 0.5mg/mL purified NA/LE hamster anti-mouse CD3e (clone:145-2C11, BD Pharmingen) and 0.5mg/mL anti-mouse CD28 (clone: 37.51, Invitrogen), and then incubated overnight at 37°C with 5% CO_2. Spleens (wild type, *Casp1*$^{-/-}$) isolated from mice were homogenized into single splenocyte

suspensions by using a 40 µm cell strainer followed by erythrolysis as described above. T cells were purified from splenocytes using a negative selection kit (*MagniSort*, Thermo Fisher) according to the manufacturer's instructions. Purity was reliably ≥ 90 % as assessed by flow cytometry. Cells were resuspended in complete RPMI1640 (Gibco) and supplemented with 10% FBS, 1 % penicillin/streptomycin and 10 µM β-mercaptoethanol. T cells were seeded into the CD3/CD28 coated plates at a density of 300,000 cells per well in a total volume of 200 µl.

BMDM – T cell co culture assays. Differentiated BMDMs were cultured for 8-10 days, then harvested, washed, counted, and seeded in flat-bottom tissue-culture treated 96-well plates at a density of 100,000 cells per well in a total volume of 200 µl, and then cultured overnight for 16 h. BMDMs were primed for 4 h with LPS (100 ng/ml). Then BMDMs were stimulated for 10 minutes with serum from either stroke or sham operated wild type mice at a concentration of 25% total volume. Control-treated BMDMs received only FBS-containing culture media. After stimulation, the culture medium was removed, and the cells were washed with sterile PBS to ensure no leftover serum in the medium. BMDM-T cell interaction was then assessed with two approaches: **1**. Stimulation by secreted factors (left), and **2**. Cell-cell contact (right). **1**: Serum-free RPMI was added to the BMDMs, which were then incubated for 1 hour at 37 °C with 5 % CO_2. The BMDM-conditioned supernatant was then transferred onto purified, cultured T cells and incubated for 2 hours at 37 °C with 5 % CO_2. **2**: T cells were added to the serum-stimulated BMDMs at a density of 200,000 cells per well in a total volume of 200 µl complete RPMI medium (10% FBS, 1 % penicillin/streptomycin and 10 µM β-mercaptoethanol), and then incubated for 2 hours at 37 °C with 5 % CO_2. T cell counts and survival rate were assessed by flow cytometry.

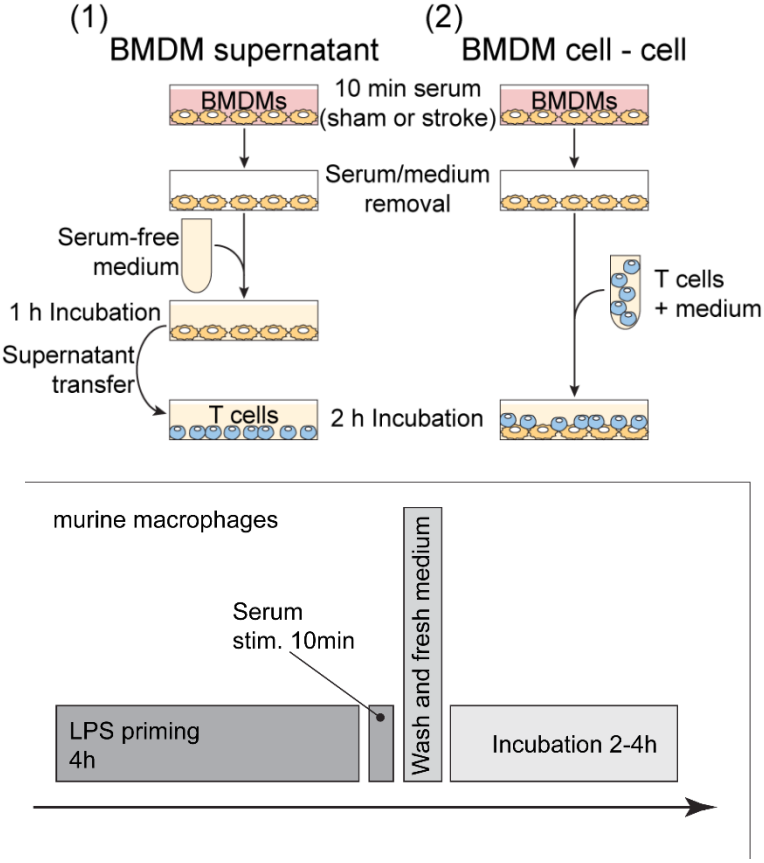

For the kinetic analysis of T cell death, we used either eGFP-actin^{+} T cells (Figure 4G: co-culture with WT or *Aim2*$^{-/-}$ BMDMs) or analyzed PI uptake of T cells after addition of PI in a final concentration of 1 µg/ml to the co-culture medium (Figure 1F: WT or *Fas lpr* T cells in co-culture with WT BMDMs). Microphotographs (10x magnification) of the cultured cells were acquired every 30 minutes for 180 minutes, starting after addition of T cells to the serum-stimulated BMDMs. Reduction in the

number of eGFP-actin$^+$ T cells or number of PI$^+$ T cells, respectively, was quantified and normalized to the corresponding control group (sham serum treated).

Immunoblotting. Spleens were harvested from deeply anaesthetized mice,and the whole organs were processed into single cell suspensions as described above. Single cell suspensions were lysed with RIPA lysis/extraction buffer with added protease/phosphatase inhibitor (Thermo Scientific, US). The total protein content of each sample was measured via bicinchoninic acid assay (Thermo Fisher Scientific, US). Whole cell extracts were fractionated by SDS-PAGE and transferred onto a polyvinlyidene difluoride membrane (BioRad, Germany). After blocking for 1 hour in TBS-T (TBS with 0.1 % Tween 20, pH 8.0) containing 4 % skim milk powder (Sigma, Germany), the membrane was washed with TBS-T and incubated with the primary antibodies against caspase-1 (1:1000; AdipoGen, US), IL-1β (1:500; R&D systems, US) and β-actin (1:1000; Sigma, Germany). Membranes were washed three times with TBS-T and incubated for 1 hour with HRP-conjugated anti-rabbit or anti-mouse secondary antibodies (1:5,000, Dako, Denmark) at room temperature. Membranes were washed three times with TBS-T, developed using ECL substrate (Millipore, US) and acquired via the Vilber Fusion Fx7 imaging system.

Human monocyte culture stimulation with human serum. Human monocytes ($3x10^5$/well) were seeded in 96 flat bottom plates with 50 ng/ml recombinant human M-CSF in RPMI 1640 (Gibco, US) supplemented with 2.5% (v/v) human serum (Sigma-Aldrich, Germany), Penicillin-Streptomycin (100 IU/ml, Thermo Fisher Scientific), Pyruvate (1 mM, Gibco) and HEPES (10 mM, Sigma-Aldrich, Germany) overnight to adjust the cells. Next day, cells were replaced with fresh medium (without M-CSF) in presence or absence of Pam3CSK4 (2.5 µg/ml) for 2 hours. Next, cells were stimulated with either control serum or stroke serum (1:4 dilution). After 2 hours, medium was gently removed and cells were washed once with PBS and replaced with fresh medium (150 µl each well) for 6 hours.

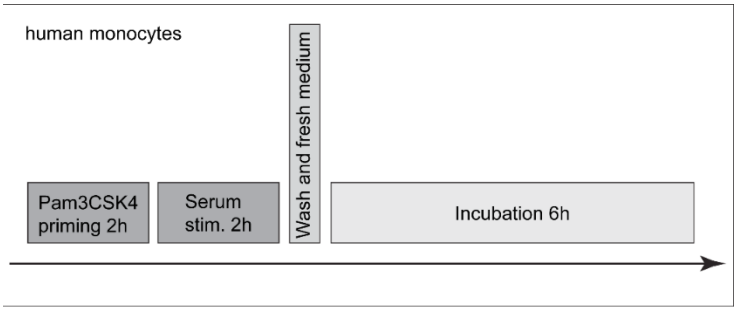

Nigericin (Sigma) was used as positive control at final concentration 6.5 µM, stimulated for 6 hours. For each condition, 5 wells were stimulated. Supernatants were collected and 50 µl from each well was used for human IL-1β ELISA (BD Biosciences, US) while remaining supernatants were combined and used for immunoblot analysis after precipitating with methanol/chloroform. Cells were directly lysed in 1X SDS Laemmli buffer and lysates were combined from 5 wells for each condition. Samples were heated at 95°C with 1100 rpm and loaded on SDS-PAGE gel (5% stacking gel and 12% separating gel; BioRad, Germany). Afterward, proteins were transferred on nitrocellulose membrane

(GE healthcare) for 1 h. Membranes were blocked for another 60 min in 3% milk in PBST (PBS containing 0.05% Tween 20). All primary antibodies of caspase-1 (1:1000; AdipoGen, US), IL-1β (1:500; R&D systems, US) were incubated at least overnight in 1% milk in PBST at 4°C. Next day, membranes were incubated for at least 1 h in secondary antibody (Santa Cruz) and washed gently in PBST buffer for further 30-60 min. Loading control β-actin-HRP antibody was purchased from Santa Cruz (1:3000). Chemiluminescent signal was recorded with CCD camera in Fusion SL (PEQLAB). Serum was obtained from patients with the following characteristics:

	Sex	Age (years)	Infarct volume	Time after symptom onset
Control	female	64	n.a.	n.a.
Stroke	female	87	161ml	7.8 hours

Free nucleic acid quantification. Cell-free nucleic acids (RNA, single strand (ss) DNA and double strand (ds) DNA) concentrations in the plasma of mice and human patients was assessed with a Qubit 2.0 fluorometer (Invitrogen) using specific fluorescent dyes which bind either ssDNA (ssDNA Assay Kit, Thermo Fisher Scientific, US) or dsDNA (HS dsDNA Assay kit, Thermo Fisher Scientific, US). Dilutions and standards were generated following the manufacturer's instructions (Thermo Fisher scientific, US).

Enzyme linked immunosorbent assay (ELISA). Total IL-1β and caspase-1 concentrations from patient plasma samples (diluted 1:10 in sterile PBS) were obtained using commercial assay kits according to the manufacturer's instructions (Quantikine ELISA human IL-1β, Quantikine ELISA human caspase-1 R&D systems, US). Total IL-1β and IL-18 concentrations from murine plasma samples were measured using the Duoset ELISA IL-1β and the Duoset ELISA IL-18 kit according to the manufacturer's instructions (R&D systems, US).

Multiplex mouse cytokine quantification. Plasma samples from mice were used to assess cytokine and chemokine concentrations (IL-1α, IL-1β, IL-2, IL-3, IL-4, IL-5, IL-6, IL-9, IL-10, IL-12(p40), IL-12(p70), IL-13, IL-17, Eotaxin, G-CSF, IFN-γ, KC, MCP-1, MIP-1α, MIP-1β, RANTES, Tnf-α) using a Luminex-100 system following the instructions in the manufacturer's manual (Bio-Plex23 Pro Mouse Cytokine Grp1, BioRad, Germany).

Infarct volumetry. Mice were euthanized by overdose of ketamine-xylazine and perfused intracardially with normal saline. Brains were removed and immediately frozen in powdered dry ice. Frozen brains were fixed in cryotech solution (OCT, tissue-tek, US) and 20 µm coronal sections were collected at 400 µm intervals. Sections were stained with cresyl violet and scanned at a resolution of 600 dpi. Infarct area of each section was assessed by ImageJ software (NIH, US). The Swanson method was employed to measure the infarct area and to correct for cortical swelling: [ischemic area]

= [area of the contralateral hemisphere] - [nonischemic area of the ipsilateral hemisphere]. The total infarct volume was determined by integrating measured areas and distances between sections.

Quantification and statistical analysis

Data were analyzed using GraphPad Prism version 6.0. All summary data are expressed as the mean ± standard deviation (s.d.) unless indicated otherwise. All data sets were tested for normality using the Shapiro-Wilk normality test. The groups containing normally distributed independent data were analyzed using a two-way Student's t-test (for 2 groups) or ANOVA (for >2 groups). Normally distributed dependent data (i.e. in vitro co-culture kinetics) were analyzed using a 2-way ANOVA. The remaining data were analyzed using the Mann-Whitney U test (for 2 groups) or Kruskal-Wallis Test (H-test, for > 2 groups). Similar variance was assured for all groups, which were statistically compared. P-values were adjusted for comparison of multiple comparisons using Bonferroni correction or Dunn's multiple comparison tests. A p value <0.05 was considered to be statistically significant.

For statistical analysis of human patient data (Fig. 5), values for dsDNA, IL-1β and lymphocyte counts were log10 transformed. We applied linear regression analysis to assess associations of serum dsDNA concentrations, IL-1β concentrations, and lymphocyte counts and logistic regression analysis to assess association with secondary infections. Where indicated, adjustment was performed for age and sex. Mediation analysis was performed using the template described by Baron and Kenny and the method by Vanderweele and Vansteelandt (Baron and Kenny, 1986; Vanderweele and Vansteelandt, 2010). All pathways were assessed using multivariable logistic regression analyses adjusting for age, sex, and dsDNA concentrations. Statistical analyses were performed in R, version 3.5.1.

Key resource table

REAGENT or RESOURCE	SOURCE	IDENTIFIER
Antibodies		
Anti-mouse CD3e (FITC/APC; 17A2)	Invitrogen	11-0032-82 / 17-0032-82
Anti-mouse CD4 (PerCP-Cy5.5; RM4-5)	Invitrogen	46-0042-82
Anti-mouse CD8a (PE; 53-6.7)	Invitrogen	12-0081-82
Anti-mouse CD19 (APC-Cy7; eBio1D3)	Invitrogen	25-0193-82
Anti-mouse CD11b (PerCP-Cy5.5/PE-Cy7; M1/70)	Invitrogen	45-0112-82 / 25-0112-82

Anti-mouse CD45 (eFluor450; 30-F11)	Invitrogen	48-0451-82
Anti-mouse CD178 (APC; MFL3)	Invitrogen	12-5911-82
Anti-mouse CD178 (InVivoMAb; MFL3)	BioXcell	BE0319
Anti-mouse IL-1beta (InVivoMAb; B122)	BioXcell	BE0246
Anti-mouse NA/LE hamster purified CD3e	BD Pharmingen	553057
Anti-mouse CD28 (funct. grade / purified)	Invitrogen	16-0281-82
Anti-mouse caspase-1 (p20; CASPER1; mouse)	Adipogen	AG-20B-0042-C100
Anti-mouse actin (rabbit)	Sigma	A2066-2ml
Anti-mouse IgG (goat, HRP-conjugated)	Dako	P0447
Anti-rabbit IgG (goat, HRP-conjugated)	Dako	PI-1000
Anti-human IL-1beta/IL-1F2	R&D systems	AF-201-NA
Anti-human caspase-1 (p20, BALLY-1; mouse)	Adipogen	AG-20B-0048-C100
Biological Samples		
Ischemic stroke patient + HC serum	LMU University Hospital Munich (Germany)	(please see details in method section)
Burn injury patient + HC serum	BG Trauma Center Ludwigshafen (Germany)	(please see details in method section)
Chemicals, Peptides, and Recombinant Proteins		
DMEM+GlutaMAX (4.5g/l D-Gluc. / Pyruvate)	Gibco	31966-021
Fetal calf serum (FCS)	Gibco	105000-064
Gentamycin (50mg/ml)	Gibco	15750-045
RPMI 1640 (L-Glutamine / 25mM HEPES)	Gibco	52400-025
Penicilin / Streptomycin	Gibco	15140-122
LPS from E.coli	Adipogen	IAX-100-013-M001

Nigericin	Adipogen	AG-CN2-0020-M025
Human recombinant DNase I	Roche	4716728001
Murine recombinant IL-1beta	R&D systems	401-ML
Caspase-1 inhibitor (VX-765, Belnacasan)	Invivogen	Inh-vx765i-1
Caspase-8 inhibitor (Z-IETD-FMK)	R&D systems	FMK007
Caspase-9 inhibitor (Z-LEHD-FMK)	R&D systems	FMK008
Beta2-adrenoreceptor inhibitor (ICI-118,551)	Sigma	5052750001
Propidium Iodide	eBiosciences	00-6990-42
beta-mercaptoethanol	Merck	M6250
RIPA lysis buffer (+protease/phosphatase inhibitor)	Thermo Fisher Sci	89900
human serum (heat-inactivated)	Sigma	H3667
Pam3CSK4	Adipogen	AG-CP3-0003-M002
Critical Commercial Assays		
Bio-Plex Pro Mouse Cytokine Grp I panel 23-Plex	BioRad	M60009RDPD
Quantikine ELISA human IL-1beta	R&D systems	DLB50
Duoset ELISA murine IL-1beta	R&D systems	DY401-05
Duoset ELISA murine IL-18	R&D systems	DY7625-05
HS dsDNA Assay Kit	Thermo Fisher Sci	Q32851
ssDNA Assay Kit	Thermo Fisher Sci	Q10212
FAM-YVAD-FMK (FAM FLICA, Caspase-1 activity)	BioRad	ICT098
T cell enrichment *MagniSort*	Thermo Fisher Sci	8804-6820-74
Streptococcus pneumoniae TIGR4	ATCC	ATCC® BAA-334™
Klebsiella pneumoniae subsp. pneumoniae	ATCC	ATCC®43816™
Experimental Models: mouse strains		
C57BL6/J	Charles River	000664

MRL/MpJ-Fas^{lpr}/J	Charles River	000485
C57BL/6-Tg(CAG-EGFP)10sb/J	Charles River	003291
Aim2$^{<tm1.2Arte>}$	Insitute for innate immunity, Bonn (Ger)	MGI:5823433
B6N.129S2-Casp1$^{<tm1Flv>}$/J	Charles River	016621
B6.129S5-Pycard^{tm1Vmd}	Gene Centre, LMU, Munich (Ger)	(Available at CR: 013189)
Myeloid ASC-KO (Lyz2-cre x Pycard$^{fl/fl}$)	BIOSS, Freiburg (Ger)	
B6. Cg-Gt(ROSA)26Sor$^{tm1.1(CAG-Pycard/mCitrine*,-CD2)Dtg}$/J	Charles River	030744
NOD.129S7(B6)-*Rag-1*$^{tm1Mom/J}$	Charles River	003729
Software and Algorithms		
BD FACSuite	Beckton Dickinson	
Amnis IDEAS v6.2	Luminex Corp.	
Microsoft Excel	Microsoft Corporation	
FlowJo v.10.6	Treestar Inc.	
GraphPad Prism 6	Graphpad SoftwareInc	
Creative Suite 6	Adobe	